

FoGE: Fock Space inspired encoding for graph prompting

Sotirios Panagiotis Chytas
University of Wisconsin-Madison
chytas@wisc.edu

Rudrasis Chakraborty
Lawrence Livermore National Lab
rudrasischa@gmail.com

Vikas Singh
University of Wisconsin-Madison
vsingh@wisc.edu

Abstract

Recent results show that modern Large Language Models (LLM) are indeed capable of understanding and answering questions about structured data such as graphs. This new paradigm can lead to solutions that require less supervision while, at the same time, providing a model that can generalize and answer questions beyond the training labels. Existing proposals often use some description of the graph to create an “augmented” prompt fed to the LLM. For a chosen class of graphs, if a well-tailored graph encoder is deployed to play together with a pre-trained LLM, the model can answer graph-related questions well. Existing solutions to graph-based prompts range from graph serialization to graph transformers. In this work, we show that the use of a parameter-free graph encoder based on Fock space representations, a concept borrowed from mathematical physics, is remarkably versatile in this problem setting. The simple construction, inherited directly from the theory with a few small adjustments, can provide rich and informative graph encodings, for a wide range of different graphs. We investigate the use of this idea for prefix-tuned prompts leveraging the capabilities of a pre-trained, frozen LLM. The modifications lead to a model that can answer graph-related questions – from simple graphs to proteins to hypergraphs – effectively and with minimal, if any, adjustments to the architecture. Our work significantly simplifies existing solutions and generalizes well to multiple different graph-based structures effortlessly.

1 Introduction

Large Language Models (LLMs) excel at tasks like question answering, sentence completion, translation, and even solving undergraduate-level math problems [1, 2]. However, they sometimes need additional data unavailable during training. For instance, a model trained on data up to a specific date may struggle with the ever-changing news cycle [3, 4]. To prevent responses from becoming outdated, or to integrate non-public/proprietary data and domain-specific terminology, models need extra context. Retrieval Augmented Generation (RAG) describes this process of retrieving and integrating extra information to an LLM during its generation process. While multiple different approaches have been proposed for the retrieval part, the most common solution to the integration of the additional information is In-Context Learning (ICL) [5, 6, 7, 8, 9].

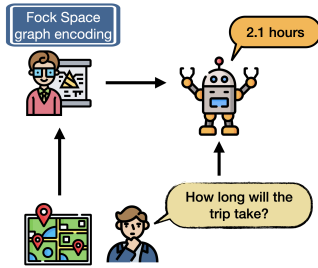


Figure 1: Augmenting LLM’s capabilities by prompting them with carefully encoded graphs.

ICL allows additional information to be included with a prompt, guiding the model to generate responses aligned with the extra context. This method is beneficial as it does not require retraining the LLM and can be applied to proprietary models like GPT [10] by adding a text description of the extra information.

ICL-type ideas are also being studied for utilizing not just additional/new data but also novel input formats/modalities, such as tables and graphs [11, 12, 13, 14]. While specialized models will still perform better at specific tasks, LLMs can serve as general-purpose reasoning machines, capable of answering questions about the provided modality beyond the training labels. Several recent results have reported success at “serializing” such structured data-types into a text-form description that can be easily used within ICL. For tables, the serialization is not too complicated [11, 12], but more care is needed for graphs. While different types of graphs can all be handled by the same pipeline, the efficacy of the model varies [15, 13, 14]. Further, it has been observed that specific design choices to “textify” the graph can influence performance and additionally, prompting techniques can have more than a small impact on results [15]. What will work well in a specific setting depends on both the question at hand as well as the characteristics of the data [16, 17].

Prefix-tuning. One option to address the issues above is “prefix-tuning” [18]. A specialized graph encoder translates the underlying graph into embeddings that can be fed directly to an LLM, removing the need for a text description. Although not training-free, the LLM remains *frozen*, and only the *relatively smaller* graph encoder is trained. This approach works well, often surpassing ICL-based methods [19, 20, 21]. However, using a specialized graph encoder can be challenging due to the *variety* of graph types, and multiple works have proposed modifications of GNNs that suit their needs. For example, GraphToken [16] can encode only simple graphs, while GNP [22] constructs a complex pipeline to handle large graphs and extract subgraphs. GraphLLM [17] combines a transformer and a GNN (about 100M parameters), requiring detailed text descriptions for each node. Adapting these models to different graph types (e.g., protein-derived graphs or hypergraphs) is difficult; even familiar graph types need adjustments for new tasks.

Context of this paper. ICL-based approaches for graphs primarily involve converting graphs to text, while prefix-tuning with graphs uses modules to extract richer, *task-relevant* structures, requiring larger sample sizes and more compute. A key question is whether we can achieve powerful, task-agnostic graph representations that are as easy to obtain as ICL-based methods. Could a lightweight adapter map these rich (but task-independent) representations into the LLM embedding space, making prefix-tuning effective for various tasks? Recent results hint that this may be viable [23]. For instance, a *single linear layer* can transform an arbitrary image encoder’s outputs to align with CLIP’s [24] text encoder embeddings. If our graph encoding captures the graph’s information and structure well enough, a similar adapter could work with a pre-trained LLM to offer good performance. This approach’s success depends on the quality of the graph representations. We ensure this by invoking a mature concept from mathematical physics, called Fock Spaces, whose practical instantiation yields almost lossless task-agnostic graph embeddings. Our findings show that a linear adapter with these representations yields competitive performance, handling complex graph questions and diverse structures like hypergraphs and proteins. The **main contribution** of this paper is the Fock-space inspired encoding of diverse graph-based structures, ranging from simple graphs to those obtained from proteins. We provide open-source code for grounding LLMs using our graph encodings as prompts and profile the performance of this pipeline relative to baselines, on diverse datasets.

2 Deriving Fock space based Graph Representations

We will first review a few notations and results which will together provide the conceptual pipeline for obtaining our representations of graphs for prompting. While graphs serve as representative examples here, the rationale for other types of structured data such as tables is similar.

Setup/rationale. Consider a graph $G = (V, E)$ with a vertex set V and an edge set E ; $|\cdot|$ denotes set cardinality. We define the *incidence matrix* [25], I to be of shape $|V| \times |E|$ where $I_{ij} = 1$ if *edge j ends at vertex i* , -1 if *edge j starts at vertex i* and 0 elsewhere. Let $|V| = n$. It is common to represent graphs via graph spectra derived from the Laplacian’s eigenvalues. This is effective for studying global properties of graphs like connectivity/symmetries (e.g., Courant Fischer theorem, Fiedler’s theorem [26, 27]) but less so for capturing localized relationships between individual entities (nodes, edges, faces) within the graph. It turns out that an interesting direction using Clifford Algebra,

shown to be effective in geometric problems in machine learning [28, 29, 28, 30, 31], provides rigorous tools for representing various graph elements (nodes, edges, faces) in a nice algebraic structure [32] **at once**. Why? Graphs can be embedded and manipulated in a geometric space [33], and in principle, their spectral properties can also be studied. We briefly summarize the concept to lay out its benefits and challenges.

2.1 Clifford Algebra and Graph Representations

Clifford Algebra. We start with a vector space W over a field K (think of \mathbb{C} for our graph setting). Vectors in W support operations like addition, scalar multiplication, and subtraction. We also equip W with an inner product $\langle \cdot, \cdot \rangle$ that measures relationships between vectors. On top of our vector space W , we construct the exterior algebra $T(W)$. This algebraic structure captures all possible products of vectors from W —including individual vectors, pairs of vectors multiplied together, triplets, and so on, along with their scalar multiples and sums. For creating the Clifford Algebra, the main insight is to modify this exterior algebra by imposing a specific constraint. We define an ideal $I(W)$ —essentially a “filter”—generated by expressions of the form $w \otimes w + \langle w, w \rangle \mathbf{1}$. Here, $w \otimes w$ is a vector multiplied by itself, and $\mathbf{1}$ is the multiplicative identity. This ideal has a closure property: multiplying any element from $I(W)$ with any element from $T(W)$ yields another element in $I(W)$.

Definition 2.1. Let W be a vector space over a field K , equipped with a quadratic form $q : W \rightarrow K$. The **Clifford algebra** of (W, q) , denoted $\mathfrak{Cl}(W, q)$, is the quotient algebra $T(W)/I(W, q)$.

Essentially, we take the exterior algebra $T(W)$ and “divide out” the ideal $I(W)$. This filters out redundant information while giving new multiplication rules that will be essential for encoding graph structure. A more in-depth analysis is available in [34, 35].

One choice of Clifford Algebra representation. A representation of a K -algebra is a homomorphism ρ that maps algebra elements to linear operators. For our Clifford algebra $\mathfrak{Cl}_n(\mathbb{C}, q)$, we use a representation $\rho : \mathfrak{Cl}_n(\mathbb{C}, q) \rightarrow \text{Hom}(W, W)$ that maps Clifford elements to linear operators on W . This allows us to manipulate abstract Clifford algebra elements as concrete matrices, which will be essential for our practical implementation.

Practical Considerations in Clifford Algebra operations. Following Clifford algebra axioms exactly allows us to build higher-order elements (like edges, hyperedges) while preserving graph structure. However, full implementation faces practical issues: an n -dimensional space requires a 2^n -dimensional Clifford algebra, and software support for high dimensions remains limited. Therefore, we make design choices that balance rigor with computational feasibility.

2.2 From Graphs to Clifford Algebra to Fock Spaces

Dirac operator. For graph G , we define the Graph Laplacian as $\Delta = II^T \in \mathbb{R}^{|V| \times |V|}$, where I is the incidence matrix of G [36]. Given the spectral decomposition $\Delta = Q\Lambda Q^T$, where $Q \in \mathbb{R}^{|V| \times |V|}$ is orthogonal and $\Lambda = \text{diag}(\lambda_1, \dots, \lambda_{|V|})$ is diagonal with eigenvalues $\lambda_i \geq 0$, we define the Dirac operator as: $D = Q\sqrt{\Lambda}Q^T \in \mathbb{R}^{|V| \times |V|}$. We express D in terms of a finite basis expansion: $D = \sum_{k=1}^{|V|} E_k \otimes \frac{\partial}{\partial e_k}$, where $e_1, \dots, e_{|V|}$ is the standard basis for $\mathbb{R}^{|V|}$. The coefficient matrices $E_k \in \mathbb{R}^{|V| \times |V|}$ capture the structure of D in each coordinate direction: $E_k = D \cdot \text{diag}(e_k)$

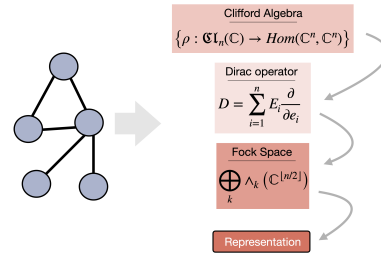


Figure 3: From graph to Fock space representations.

Connection to Clifford Algebra. The coefficient matrices E_k generate a representation of the Clifford algebra $\mathfrak{Cl}(\mathbb{R}^{|V|}, q)$. Specifically, they satisfy: $E_i E_j + E_j E_i = -2q(e_i, e_j) \text{Id}_{|V|}$ where $q(e_i, e_j)$ denotes the quadratic form evaluated on basis elements and Id is the identity matrix.

Connection to differential geometry. This discrete formulation parallels the continuous case in differential geometry. The Dirac operator D acts differently depending on the function type: for real-valued functions, $(Df)(v)$ gives a weighted average of neighboring vertex values; for vector-valued functions, D acts independently on each component; for complex-valued functions, D incorporates phase information; and for spinor-valued functions, D acts on $\mathcal{S}(G)$ with complex matrices D_{vw} . This quantum mechanical connection will give useful heuristics for our approach shortly.

Spinors and Fock space. For the complex Clifford Algebra, there exists an irreducible representation $\phi : \mathcal{Cl}_{|V|}(\mathbb{C}, q) \rightarrow \text{End}(\mathbb{S})$, where $\text{End}(\mathbb{S})$ denotes the space of linear endomorphisms of \mathbb{S} , and \mathbb{S} is a complex vector space of dimension $2^{\lfloor |V|/2 \rfloor}$, called the Spinor space [35]. Note that $\text{End}(W)$ and $\text{Hom}(W, W)$ are essentially the same object. The **Spinor** space is relevant because of the following crucial result: the Spinor space \mathbb{S} can be identified with the exterior algebra $\wedge(\mathbb{C}^{\lfloor |V|/2 \rfloor})$, which is isomorphic to the **Fock space** $\mathbb{F} = \bigoplus_{k=0}^{\lfloor |V|/2 \rfloor} \wedge^k(\mathbb{C}^{\lfloor |V|/2 \rfloor})$. This isomorphism allows us to work with the Fock space representation instead of the complete Clifford algebra.

Why is this useful? The Dirac operator uses only the basis elements E_k of the Clifford algebra. These basis elements act on spinors, which can now be identified with elements of the Fock space. The key insight is that the action of E_k on the Fock space can be decomposed into creation and annihilation operators: $E_k \simeq a_k + a_k^*$ where a_k is the annihilation operator and a_k^* is the creation operator. This decomposition is important for a few reasons. First, creation and annihilation operators provide an intuitive interpretation: creation operators a_k^* add “particles” to states, while annihilation operators a_k remove them. In our graph context, this means adding or removing structural elements. Second, working with these operators avoids the complexity of implementing the full Clifford algebra or the full Spinor space (dimension $2^{\lfloor |V|/2 \rfloor}$). We can work with much simpler operations – and use heuristic substitutes for the creation and annihilation operators.

2.3 Translating Theory to Practice: Instantiating a Graph Representation

The Fock space formulation provides ideas for representing multi-particle systems, thinking of particles as nodes in a graph. As noted above, implementing the full structure, in high dimensions, is challenging. Vector Symbolic Architectures (VSA), as explored in recent works [37, 38], offer a practical approximation of Fock spaces with compute efficiency. In VSA, the binding operation (circular convolution) approximates the creation/annihilation operators, while the superposition operation (vector addition) resembles the direct sum in Fock spaces. Although the VSA \leftrightarrow quantum mechanics connection is not new [39], but in this context, it provides specific ideas for efficiency.

Representing nodes, sums, and products. In our implementation, we assign a high-dimensional vector to each concept (node, edge, and so on). These vectors play a role analogous to the basis elements in the expansion of the Dirac operator. While ideally, these vectors would be orthogonal, similar to the properties of basis elements in a Fock space, we simply approximate this by sampling from a normal distribution $\mathcal{N}(0, 1/d)$. This leads to nearly orthogonal vectors, with the maximum absolute cosine similarity between any two vectors typically below 0.1 [40].

To emulate operations in Fock space, we use dimensionality-preserving operations instead of tensor products, avoiding exponential growth in dimensionality [39]. This ensures all embeddings maintain the same dimensionality. We define sum (\oplus) as element-wise addition and product (\otimes) as circular convolution, analogous to Fock space’s creation/annihilation operators. Circular convolution is done via element-wise multiplication in the Fourier domain followed by an inverse Fourier transform. As d increases, these operations asymptotically satisfy Fock space’s algebraic properties, with complexity $\mathcal{O}(d \log d)$. This framework also supports inverse vectors, where $a \otimes b = \mathbf{1}$. Other properties like commutation relations, superposition, and self-commutation are mostly satisfied. Note that our experiments are not tied to this specific implementation (improved choices can be dropped in).

Dealing with infinitely many concepts. In some datasets, vertices include text descriptions, making random vector initialization unsuitable. To address this, we use text encoders like CLIP [24], BERT [41], and RoBERTa [42], which map text to vectors that preserve information and place similar sentences in close proximity. This approach allows us to: (1) generate infinitely many vectors, and (2) ensure similar vectors represent similar concepts. When dimensionality allows, we retain default sampling and explicitly note the use of text encoders in our experiments.

Other works using Vector Symbolic Architectures. Vector Symbolic Architecture (VSA), rooted in symbolic AI, leverages high-dimensional representations alongside logical rules for combining symbols/vectors [43]. Many studies mechanistically derive ways to construct symbols and implement merge operations. The use of Fock space for symbolic manipulation has been explored, with applications in trajectory analysis [39]. Additionally, vector symbolic representations have been employed for computational efficiency in self-attention calculations, as seen in HRRFormers [44, 37].

3 Fock Graph Encoder (FoGE)

Based on the concepts from §2, we use a parameter-free scheme (denoted FoGE) to obtain rich graph embeddings. Our approach is general and can handle a large spectrum of different graph types, and its extension to novel graph-types is straightforward. Diverse graph types such as hypergraphs, attributed graphs, as well as proteins (Fig. 4) can all be modeled easily providing an alternative or a good initialization for more intensive trainable models. This approach translates the concepts of Fock spaces into a practical/efficient method for graph representation, where graph features obtained by the encoding are analogous to multi-particle states in a Fock space.

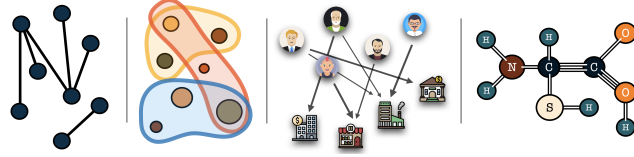
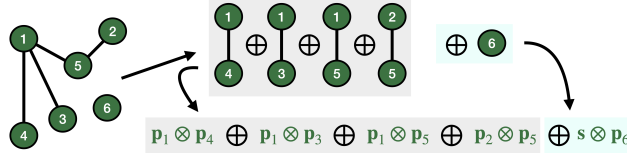


Figure 4: Graphs, Hypergraphs, Attributed graphs, Proteins. All these types can be efficiently encoded using FoGE.

For a graph $G = (V, E)$ we have a set of vectors $[\mathbf{p}_i]_{i=1}^{n=|V|}$, using i to index the nodes. We also use an extra vector \mathbf{s} for the graph’s size, a practical design choice we will explain shortly. Then, with these $n + 1$ vectors, we obtain a lossless Fock-space based representation \mathbf{g} as:

$$\mathbf{g} = (\mathbf{s} \otimes \mathbf{p}_n) \oplus \bigoplus_{(i,j) \in E} (\mathbf{p}_i \otimes \mathbf{p}_j) \quad (1)$$

Our formulation follows from §2. Each edge’s endpoints are fused together using \otimes and then we aggregate all edges together using \oplus . Finally, the graph’s size is also added using the special vector \mathbf{s} .



Lossless representation. The above representation is lossless. Assuming we use (1) to get a graph’s embedding \mathbf{g} . Then, simply by evaluating the expression $\mathbf{p}_j^T (\mathbf{p}_i^{-1} \otimes \mathbf{g})$, we can determine whether the edge (i, j) exists in the edge set of that particular graph. In this way, we can recover, one by one, all edges of the graph and correctly reconstruct it, if desired. It is instructive to check the importance of \mathbf{s} . By evaluating the expression $\mathbf{p}_i^T (\mathbf{s}^{-1} \otimes \mathbf{g})$, $\forall i$, we can first obtain the size of the graph. This can inform the edge retrieval above because an expression of the form $\mathbf{p}_{n+x}^T (\mathbf{p}_i^{-1} \otimes \mathbf{g})$ could, in practice, produce a number close to 1, although there is no such edge. By first obtaining the size of the graph, we have a “safeguard” against such phantom edges beyond the real vertex-set.

Vertex attributes. Consider a graph $G = (V, E, Attr)$, where the set $Attr$ (with $|Attr| = |V|$) consists of attributes, one for each vertex. There is no restriction on the type of attributes: it can denote numerical values or text or any other concept. Let \mathbf{a}_i be the vector associated with the attribute of vertex $i \in V$ (using an appropriate text-encoder if needed). Then, we can augment (1) to absorb the extra information in the following way:

$$\mathbf{g} = (\mathbf{s} \otimes \mathbf{p}_n) \oplus \bigoplus_{(i,j) \in E} (\mathbf{p}_i \otimes \mathbf{p}_j) \oplus \bigoplus_{i \in V} (\mathbf{p}_i \otimes \mathbf{a}_i) \quad (2)$$

The graph is again, fully reconstructable. We have also encoded each vertex’s attribute (which can be recovered by the expression $\mathbf{a}_j^T (\mathbf{p}_i^{-1} \otimes \mathbf{g})$). We should think of proteins as a graph with vertex attributes where each vertex is a specific amino acid (possibly with 3-D coordinates).

Hypergraphs (Theory versus Practice). Hypergraphs are generalizations of graphs: each edge is connected to an arbitrary number of vertices, instead of just 2 (Fig. 4). In theory, we can easily augment (1) so that we can handle hypergraphs as follows:

$$\mathbf{g} = (\mathbf{s} \otimes \mathbf{p}_n) \oplus \bigoplus_{(k_1, \dots, k_m) \in E} \bigotimes_{i=1}^m \mathbf{p}_{k_i} \quad (3)$$

In practice, aggregating many multiple vectors together may be unstable. This is true for our particular design choices for calculations (e.g., circular convolution), so we use an alternative approach. We can start by observing that each edge can be interpreted as a unique cluster of vertices, so we simply assign a unique vector \mathbf{e}_i , $i \in [|E|]$ to each edge in the hypergraph. This modification allows us to encode the hypergraph similar to how a graph is encoded as a dictionary, in the following way:

$$\mathbf{g} = (\mathbf{s} \otimes \mathbf{p}_n) \oplus \left(\bigoplus_{i=1}^{|E|} \left(\mathbf{e}_i \otimes \bigoplus_{j \in E_i} \mathbf{p}_j \right) \right) \quad (4)$$

3.1 Fock Space-based grounding of LLMs (FoGE-LLM)

Recent works showed that (a) textualizing a graph and pre-appending it to a question results in better-than-random responses from the LLM (although far from perfect), and (b) using a specialized graph encoder such as a GNN or a graph transformer and training along with a frozen LLM results in a big improvement in performance, resulting essentially in LLMs that can understand, to some extent, graphical structures. One takeaway is that we can bypass the most tedious stage of designing application-specific graph encoders. Instead, we can use a **parameter-free** method for a wide range of graph types, as we described above. Thus, the *only* trainable parts of the pipeline are simple linear adapters that convert the raw graph encodings to a format “understandable” by an LLM. Our FoGE-LLM is shown in Fig. 5. After getting the graph encodings, we train one/more linear adapters and append the transformed encodings to the question’s embeddings fed to the LLM.

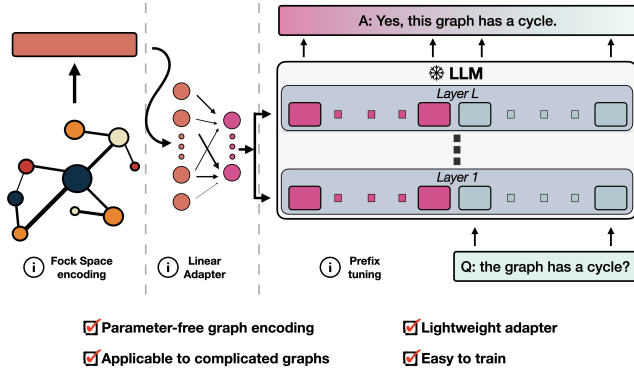


Figure 5: FoGE-LLM overview. Using a parameter-free graph encoder we get graph embeddings for a range of different graphs. Then, we use linear adapters with a frozen LLM for *prefix tuning*.

Summary and Takeaway. We highlight some key advantages. *First*, our graph encoding is parameter-free and efficient. The complexity of aggregation is $\mathcal{O}(d \log d)$ (d is vectors’ dimension) and the number of aggregation operations is linear (in graph size). *Second*, our encoder is not restricted to specific graph types: it works easily for simple graphs, for proteins and for hypergraphs just via small modifications. In contrast, GraphToken [16] uses a specific GNN whose output size is dependent on the underlying task whereas GraphLLM [17] uses a transformer model together with a GNN (also specific to the underlying task). These properties simplify our training and eliminates any tunable components. *Third*, our open-source code offers a scalable way to train FoGE-LLM even on consumer GPUs, by using FSDP [45]. For reference, GraphToken [16] is trained on TPUs (code unavailable) whereas GraphLLM [17] has a large memory/compute footprint (trained on A100 80GB).

4 Experimental results

We examine our Fock-space based encoding in two separate settings: (a) as a stand-alone input of a simple model, and (b) as an extra prefix in a frozen LLM (FoGE-LLM), for graph prompting.

Datasets and Models. We performed experiments on multiple graph reasoning datasets: from simple graph-understanding tasks to hypergraphs and proteins and aim to cover different aspects of

graph understanding/reasoning. Specifically, we consider the 6 following datasets/dataset collections: (i) **GraphQA** [15] (ii) **GraphReasoning** [17] (iii) **HyperGraphQA** (iv) **PPI** [46] (v) **OBNB** [47] (vi) **SabDab** [48]. More details about the datasets can be found in the appendix. Exploring diverse graph reasoning datasets helps evaluate our model’s performance and generalization across various graph structures and domains, from traditional graph-based QA to hypergraph understanding and biological network analysis. By including real-world datasets like PPI, BioGRID, and HumanNet, we highlight the practical relevance of our result, with potential applications in biology, network analysis, and more.

We use the Llama2 (7B) model [49] as the frozen LLM, and we use only extra linear adapters for the graph embeddings obtained using our formulation. We adjust vector dimensionality from 512 to 2048 and use just a *single adapter* for the entire model or *one adapter per layer* in FoGE-LLM.

4.1 Proof of Principle Evaluations for Graph Understanding

Setup and Results. While our key goal is graph-prompting, we first perform multiple preliminary checks of the effectiveness of our graph encoding. We conduct three different types of experiments.

First, we evaluate whether our graph embeddings are informative (i.e., they preserve the graph’s structure), by using a small, 1-hidden-layer FFN for basic and advanced graph-understanding tasks. The complete results in the appendix show that our representations are rich and informative. On simple tasks, using GraphQA [15], we demonstrate that we can answer questions such as whether a graph has a cycle with an almost perfect accuracy. For more involved tasks, we consider the Open

Graph Benchmark (OGB) [52] and we show that our encoding is better than multiple, heavy, specialized, and trainable methods but training-free and unsupervised! Additionally, because our method allows a seamless integration of additional graph information (like a molecule’s footprint), we show that this can help us achieve even better results and in some cases, be competitive with submissions at the top of the leaderboard. The detailed results are in the appendix.

Second, we examine whether our graph encodings preserve important biological markers of the data. To test this, we use a small dataset of about 900 proteins (SabDab) which are accompanied by affinity data that corresponds to each protein’s clade. Briefly, clades are protein superfamilies, based on common ancestry (more information can be found in the appendix). In principle, proteins from the same clade are *more similar* than across clades, so we examine whether this is also preserved in our obtained embeddings. Although the dataset has only few samples and some of the clades are scarcely populated, we can observe that there is a clear separation between the most populated clades in the embeddings space.

Third, we examine if the same encoding practice can generate rich node-level encodings, by encoding for each node, the subgraph that is generated by itself and its neighbors. We examine the performance in **nineteen** real protein datasets (PPI [46] and OBNB [47]) in Tables 1 and 2, while the detailed results can be found on the appendix. We see that our approach is, in all datasets, among the best unsupervised approaches, and is also competitive (if not better) than specialized

supervised approaches that leverage trainable, graph-specific models such as GCN [50] and GAT [51]. Specifically, we achieve state-of-the-art performance in PPI while we are the best-performing method (among both unsupervised and supervised) in seven out of the eighteen datasets of OBNB.

Table 1: Results on two real protein datasets from OBNB. Our method is the strongest unsupervised scheme to obtain node embeddings, especially for the DisGeNet task. Its performance is comparable to trainable, graph-specific models (GCN, GAT). More details on all baselines are in [47]. The reported metric is the APOP (Average test Precision Over Prior) over all target labels.

Model	BioGRID		HumanNet	
	DisGeNet	GOBP	DisGeNet	GOBP
LabelProp	0.931	1.885	3.059	3.806
Adj + LR	0.743	2.528	3.053	3.964
Node2Vec + LR	0.836	2.571	2.433	4.036
LapEigMap + LR	0.864	2.149	2.301	3.778
FoGE	1.062	2.433	3.254	3.916
GCN [50]	1.012	2.572	3.116	3.812
GAT [51]	1.063	2.562	3.065	3.963

Table 2: Micro F1-score on PPI. Our approach is better than the best unsupervised approaches and better/comparable to the supervised approaches.

	Model	F1
Unsupervised	Random	39.2
	Node2Vec [53]	40.9
	Raw features [53]	42.2
	GraphSAGE-min [46]	46.5
	GraphSAGE-max [46]	50.2
	DGI [54]	63.8
	GRACE [55]	66.2
	FoGE	99.2
	GraphSAGE-min [46]	50.0
	GraphSAGE-max [46]	61.2
Supervised	LGCN [56]	77.2
	GAT [51]	97.3
	GCNII [57]	99.5

These results provide encouraging evidence that (a) our approach gives “rich” graph embeddings for a range of different graph types and styles, and (b) our graph embeddings can be used as an extra, grounding input to a powerful LLM without the need to design/train a specialized model, e.g., GNN [58, 59] or a Graph Transformer [60].

4.2 Grounding LLMs with Graph prompting

Graph Understanding. In our first experiment, we examine whether an LLM can answer questions about a graph’s structure, such as the number of nodes, the presence of cycles, and so on. We use GraphToken and conduct a suite of six different experiments. Although our method’s encodings are *not* specific to each underlying task, it performs competitively with specialized models, as shown in Table 3. Even when GraphToken uses different embeddings for each node (*node degree*) or edge (*edge existence*), our model still achieves comparable results using a single embedding for the entire graph.

Table 3: GraphToken vs FoGE-LLM on GraphQA. Column 1 stands for a single embedding for the entire graph; $\mathcal{O}(n)$ stands for a single embedding per node. In all 6 tasks, although we use a parameter-free, predetermined graph encoding, we see a performance similar/better relative to a trainable graph encoder with a larger LLM.

	ICL	GraphToken		FoGE-LLM
Tokens	$\mathcal{O}(n^2)$	1	$\mathcal{O}(n)$	1
num of nodes	26.9%	99.6%	-	97.2%
num of edges	12.8%	42.6%	-	45.1%
cycle existence	83.2%	95.6%	-	97.9%
num of triangles	16.2%	34.8%	-	37.7%
edge existence	54.4%	-	73.8%	74.3%

Advanced Graph Reasoning. Going beyond “simple” graph understanding tasks, we also examine our performance on more complicated graph-reasoning tasks, using a recent dataset [17]. GraphToken is not applicable here since each node is accompanied by a textual description which cannot be handled by that model. So, our main baseline is GraphLLM, which uses a transformer combined with a GNN to merge the graphical/textual information into one or more embedding vectors. Similar to GraphToken [16], GraphLLM [17] also utilizes a different approach for each task, using multiple graph embeddings for each task. In contrast, we achieve comparable performance using a *single graph embedding*, showcasing the versatility/richness of the graph embeddings. Further, we see that using a pretrained text encoder such as RoBERTa [42] to generate the vectors is reasonable, and results in a similar performance. This is a strong improvement over traditional symbolic methods, by allowing a large set of “symbols”/vectors. Dealing with proteins is similar to advanced graph reasoning, since both datasets are graphs with additional node information. In Table 5, we show the accuracy of FoGE-LLM for three protein-related tasks on Jaffe. Although the size of the proteinic graphs is more than $10\times$ larger compared to the ones in GraphQA and GraphReasoning, our model is able, up to some extent, to understand the provided protein, as a whole (*number of amino acids* and *number of links*) as well as at an individual-node level for the task *type of amino acid* (where we prompt the model to determine the type of a specific vertex in the protein).

Hypergraphs. Existing works focus on specific forms of graphs and rarely applicable (or easily modifiable) to different graph types. One common family of graphs in applications is hypergraphs. Here each edge is a subset of the nodes, of arbitrary size (Fig. 4). Our formulation can handle such a generalization of the typical graphs with only minor modifications to the encoding formulation (Eq. 4). Here, we show that our design can indeed answer questions about such complicated structures, using our encodings as an extra prefix (graph prompting). Using the proposed dataset (HyperGraphQA), we

Table 4: GraphLLM vs FoGE-LLM. Although we are using the same, predetermined graph embedding for each task, we enjoy a performance similar to GraphLLM which leverages 5 graph embeddings, specific to the task at hand. The *vectors* stands for the two approaches we follow in generating them: (a) randomly generated (almost) orthogonal vectors (ignoring the node’s text description), and (b) using RoBERTa [42] and utilizing all vertices’ information.

	GraphLLM	FoGE-LLM	
model size	100M	25M	
question specific output	Yes	No	
graph embeddings	5	1	
vectors	-	random	RoBERTa
substructure count	99.9%	97.3%	95.6%
max triplet sum	95.7%	94.6%	94.7%
shortest path	97.2%	95.7%	95.8%
bipartite match	99.8%	98.1%	97.3%

Table 5: FoGE-LLM performance against ICL techniques for hypergraphs and proteins.

		Zero-Shot	Few-Shot	FoGE-LLM
HyperQA	num of nodes	04.5%	16.8%	85.0%
	num of edges	03.9%	27.0%	95.4%
	node degree	02.1%	10.1%	53.9%
	edge existence	65.9%	79.4%	87.9%
Jaffe	num of amino-acids	03.9%	17.1%	99.3%
	num of links	03.8%	06.1%	13.2%
	amino-acid type	01.4%	12.3%	37.7%

assess the performance of FoGE-LLM on four

common tasks. Since GraphToken as well as GraphLLM cannot handle such data, we compare our model’s performance against two of the most common prompt-engineering methods: 1. zero-shot, where the model is given the graph in text form along with the corresponding question, and 2. few-shot, where the model is given pairs of textualized graphs with the corresponding question/answer pair and it is asked to produce the answer to a new combination of graph/question. The results are presented in Table 5. Interestingly, even though hypergraphs have a much more complicated structure than “simple” graphs, our model achieves a performance very close to basic graph understanding (Table 3), or even better at some tasks.

5 Related Work

Geometric Algebra in Machine Learning. There is growing interest in application of geometric algebra in machine learning, particularly for developing networks that maintain geometric properties. While these ideas have been leveraged in the context of equivariance/symmetry transformations in deep learning [61, 62, 63, 64, 65], the theory is finding interesting uses in recent works. For example, [66] recently proposed Clifford Neural Layers to model dynamical systems in fields like fluid dynamics and [28] described Geometric Clifford Algebra Networks (GCANs), specifically designed to respect symmetry group transformations. Beyond classical machine learning, geometric algebra finds more direct applications in quantum computing as well: [67] leveraged the isomorphism between Pauli matrices and Clifford Algebra to represent multidimensional data, to define specialized transforms for machine learning tasks.

Graphs & LLMs. The body of work describing ways to infuse extra, graphical information into a frozen LLM is sizable and growing. As discussed earlier, initial approaches focused on converting the underlying graph into natural language form, such as “node 1 is connected to node 3, node 5 is connected to node 4, ...” [13, 14, 15]. These works while far from perfect showed viability: that a frozen LLM has the capability to reason about the given graph and answer graph-related questions, such as “is there a cycle in the graph?”. Practical difficulties involving the format of graph serialization is an important factor in the performance and the results tend to be only moderately better than random. The perspective taken in [16, 17] was fresh and led to an alternative approach: infusing the graph information directly at the embedding level, by encoding the graph using a model such as a Graph Neural Network (GNN) [58, 59, 16] or a Graph Transformer [60, 17]. These works significantly improved the state of the art, showing that carefully crafted graph embeddings are key to a successful grounding of an LLM.

6 Conclusions

We have described a novel strategy to encode a graph into a vector form for direct downstream use or to augment prompts fed to LLMs. Our approach, grounded in Clifford algebra and Fock space operations, is rigorous and offers numerous advantages in practice demonstrated via experiments. We can obtain encodings of arbitrary graphs instantly, with no trainable parameters, that nicely encapsulates the important information content in the underlying graph. Using these encodings, we introduced FoGE-LLM, a way to fuse the graph information for graph-prompting with a pre-trained, frozen LLM, allowing it to “understand” and reason about graphs. Our model, accompanied with a simple-to-train open-source codebase, performs favorably relative to highly specialized models while at the same time handling classes of graphs where other alternatives fall short or need adjustments.

Impact & Limitations. A key strength of our method is its parameter-free approach for generating rich graph embeddings. Such an approach can be a great fit in less computationally rich environments or in cases where the dataset’s size is not big enough for the trainable approaches, without, as we demonstrated extensively, lacking in performance in data-rich situations. Given the scarcity of the data in many real-life graph-related problems (like the protein-based questions we answered here), our approach can benefit multiple aspects of research and life. However, the unsupervised nature of FoGE also limits the ability to fine-tune performance if the embeddings are insufficient for specific applications. We suggest building representation learners on top of these embeddings, which happens in FoGE-LLM. Additionally, when dealing with infinitely large vector sets, random generation is impractical. While RoBERTa works well in our experiments, integration with other models may involve some trial-and-error to identify sensible configurations.

References

- [1] Hongwei Liu, Zilong Zheng, Yuxuan Qiao, Haodong Duan, Zhiwei Fei, Fengzhe Zhou, Wenwei Zhang, Songyang Zhang, Dahua Lin, and Kai Chen. Mathbench: Evaluating the theory and application proficiency of llms with a hierarchical mathematics benchmark. 2024.
- [2] Moa Johansson. What can large language models do for theorem proving and formal methods? In Bernhard Steffen, editor, *Bridging the Gap Between AI and Reality*, pages 391–394, Cham, 2024. Springer Nature Switzerland. ISBN 978-3-031-46002-9.
- [3] Tu Vu, Mohit Iyyer, Xuezhi Wang, Noah Constant, Jerry Wei, Jason Wei, Chris Tar, Yun-Hsuan Sung, Denny Zhou, Quoc Le, et al. Freshllms: Refreshing large language models with search engine augmentation. *arXiv preprint arXiv:2310.03214*, 2023.
- [4] Seyed Mahed Mousavi, Simone Alghisi, and Giuseppe Riccardi. Is your llm outdated? benchmarking llms & alignment algorithms for time-sensitive knowledge. *arXiv preprint arXiv:2404.08700*, 2024.
- [5] Kelvin Guu, Kenton Lee, Zora Tung, Panupong Pasupat, and Mingwei Chang. Retrieval augmented language model pre-training. In Hal Daumé III and Aarti Singh, editors, *Proceedings of the 37th International Conference on Machine Learning*, volume 119 of *Proceedings of Machine Learning Research*, pages 3929–3938. PMLR, 13–18 Jul 2020. URL <https://proceedings.mlr.press/v119/guu20a.html>.
- [6] Yujuan Ding, Wenqi Fan, Liangbo Ning, Shijie Wang, Hengyun Li, Dawei Yin, Tat-Seng Chua, and Qing Li. A survey on rag meets llms: Towards retrieval-augmented large language models. *arXiv preprint arXiv:2405.06211*, 2024.
- [7] Qingxiu Dong, Lei Li, Damai Dai, Ce Zheng, Zhiyong Wu, Baobao Chang, Xu Sun, Jingjing Xu, and Zhifang Sui. A survey on in-context learning. *arXiv preprint arXiv:2301.00234*, 2022.
- [8] Barret Zoph, Colin Raffel, Dale Schuurmans, Dani Yogatama, Denny Zhou, Don Metzler, Ed H. Chi, Jason Wei, Jeff Dean, Liam B. Fedus, Maarten Paul Bosma, Oriol Vinyals, Percy Liang, Sebastian Borgeaud, Tatsunori B. Hashimoto, and Yi Tay. Emergent abilities of large language models. *TMLR*, 2022.
- [9] Sewon Min, Xinxu Lyu, Ari Holtzman, Mikel Artetxe, Mike Lewis, Hannaneh Hajishirzi, and Luke Zettlemoyer. Rethinking the role of demonstrations: What makes in-context learning work? In Yoav Goldberg, Zornitsa Kozareva, and Yue Zhang, editors, *Proceedings of the 2022 Conference on Empirical Methods in Natural Language Processing*, pages 11048–11064, Abu Dhabi, United Arab Emirates, December 2022. Association for Computational Linguistics. doi: 10.18653/v1/2022.emnlp-main.759. URL <https://aclanthology.org/2022.emnlp-main.759>.
- [10] Tom Brown, Benjamin Mann, Nick Ryder, Melanie Subbiah, Jared D Kaplan, Prafulla Dhariwal, Arvind Neelakantan, Pranav Shyam, Girish Sastry, Amanda Askell, et al. Language models are few-shot learners. *Advances in neural information processing systems*, 33:1877–1901, 2020.
- [11] Yuan Sui, Mengyu Zhou, Mingjie Zhou, Shi Han, and Dongmei Zhang. Table meets llm: Can large language models understand structured table data? a benchmark and empirical study. In *Proceedings of the 17th ACM International Conference on Web Search and Data Mining, WSDM ’24*, page 645–654, New York, NY, USA, 2024. Association for Computing Machinery. ISBN 9798400703713. doi: 10.1145/3616855.3635752. URL <https://doi.org/10.1145/3616855.3635752>.
- [12] Weizheng Lu, Jiaming Zhang, Jing Zhang, and Yueguo Chen. Large language model for table processing: A survey. *arXiv preprint arXiv:2402.05121*, 2024.
- [13] Heng Wang, Shangbin Feng, Tianxing He, Zhaoxuan Tan, Xiaochuang Han, and Yulia Tsvetkov. Can language models solve graph problems in natural language? In A. Oh, T. Naumann, A. Globerson, K. Saenko, M. Hardt, and S. Levine, editors, *Advances in Neural Information Processing Systems*, volume 36, pages 30840–30861. Curran Associates, Inc., 2023.

- [14] Jiayan Guo, Lun Du, and Hengyu Liu. Gpt4graph: Can large language models understand graph structured data? an empirical evaluation and benchmarking. *arXiv preprint arXiv:2305.15066*, 2023.
- [15] Bahare Fatemi, Jonathan Halcrow, and Bryan Perozzi. Talk like a graph: Encoding graphs for large language models. In *The Twelfth International Conference on Learning Representations*, 2024. URL <https://openreview.net/forum?id=IuXR1CCrSi>.
- [16] Bryan Perozzi, Bahare Fatemi, Dustin Zelle, Anton Tsitsulin, Mehran Kazemi, Rami Al-Rfou, and Jonathan Halcrow. Let your graph do the talking: Encoding structured data for llms, 2024.
- [17] Ziwei Chai, Tianjie Zhang, Liang Wu, Kaiqiao Han, Xiaohai Hu, Xuanwen Huang, and Yang Yang. Graphllm: Boosting graph reasoning ability of large language model. *arXiv preprint arXiv:2310.05845*, 2023.
- [18] Xiang Lisa Li and Percy Liang. Prefix-tuning: Optimizing continuous prompts for generation. In Chengqing Zong, Fei Xia, Wenjie Li, and Roberto Navigli, editors, *Proceedings of the 59th Annual Meeting of the Association for Computational Linguistics and the 11th International Joint Conference on Natural Language Processing (Volume 1: Long Papers)*, pages 4582–4597, Online, August 2021. Association for Computational Linguistics. doi: 10.18653/v1/2021.acl-long.353. URL <https://aclanthology.org/2021.acl-long.353>.
- [19] Mingchen Sun, Kaixiong Zhou, Xin He, Ying Wang, and Xin Wang. Gppt: Graph pre-training and prompt tuning to generalize graph neural networks. In *Proceedings of the 28th ACM SIGKDD Conference on Knowledge Discovery and Data Mining, KDD '22*, New York, NY, USA, 2022. Association for Computing Machinery. ISBN 9781450393850. doi: 10.1145/3534678.3539249. URL <https://doi.org/10.1145/3534678.3539249>.
- [20] Zemin Liu, Xingtong Yu, Yuan Fang, and Xinming Zhang. Graphprompt: Unifying pre-training and downstream tasks for graph neural networks. In *Proceedings of the ACM Web Conference 2023, WWW '23*, New York, NY, USA, 2023. Association for Computing Machinery. ISBN 9781450394161. doi: 10.1145/3543507.3583386. URL <https://doi.org/10.1145/3543507.3583386>.
- [21] Jiabin Tang, Yuhao Yang, Wei Wei, Lei Shi, Lixin Su, Suqi Cheng, Dawei Yin, and Chao Huang. Graphgpt: Graph instruction tuning for large language models. In *Proceedings of the 47th International ACM SIGIR Conference on Research and Development in Information Retrieval, SIGIR '24*, page 491–500, New York, NY, USA, 2024. Association for Computing Machinery. ISBN 9798400704314. doi: 10.1145/3626772.3657775. URL <https://doi.org/10.1145/3626772.3657775>.
- [22] Yijun Tian, Huan Song, Zichen Wang, Haozhu Wang, Ziqing Hu, Fang Wang, Nitesh V. Chawla, and Panpan Xu. Graph neural prompting with large language models. *Proceedings of the AAAI Conference on Artificial Intelligence*, 38(17):19080–19088, Mar. 2024. doi: 10.1609/aaai.v38i17.29875. URL <https://ojs.aaai.org/index.php/AAAI/article/view/29875>.
- [23] Mazda Moayeri, Keivan Rezaei, Maziar Sanjabi, and Soheil Feizi. Text-to-concept (and back) via cross-model alignment. In Andreas Krause, Emma Brunskill, Kyunghyun Cho, Barbara Engelhardt, Sivan Sabato, and Jonathan Scarlett, editors, *Proceedings of the 40th International Conference on Machine Learning*, volume 202 of *Proceedings of Machine Learning Research*, pages 25037–25060. PMLR, 23–29 Jul 2023. URL <https://proceedings.mlr.press/v202/moayeri23a.html>.
- [24] Alec Radford, Jong Wook Kim, Chris Hallacy, Aditya Ramesh, Gabriel Goh, Sandhini Agarwal, Girish Sastry, Amanda Askell, Pamela Mishkin, Jack Clark, Gretchen Krueger, and Ilya Sutskever. Learning transferable visual models from natural language supervision. In Marina Meila and Tong Zhang, editors, *Proceedings of the 38th International Conference on Machine Learning*, volume 139 of *Proceedings of Machine Learning Research*, pages 8748–8763. PMLR, 18–24 Jul 2021. URL <https://proceedings.mlr.press/v139/radford21a.html>.
- [25] Allen Hatcher. *Algebraic Topology*. Cambridge University Press, 2002.

- [26] Miroslav Fiedler. Algebraic connectivity of graphs. *Czechoslovak Mathematical Journal*, 23(2): 298–305, 1973. URL <http://eudml.org/doc/12723>.
- [27] Miroslav Fiedler. Laplacian of graphs and algebraic connectivity. *Banach Center Publications*, 25(1):57–70, 1989. URL <http://eudml.org/doc/267812>.
- [28] David Ruhe, Jayesh K. Gupta, Steven De Keninck, Max Welling, and Johannes Brandstetter. Geometric clifford algebra networks. In *Proceedings of the 40th International Conference on Machine Learning, ICML’23*. JMLR.org, 2023.
- [29] Siqi Chen, Pierre-Philippe Dechant, Yang-Hui He, Elli Heyes, Edward Hirst, and Dmitrii Riabchenko. Machine learning clifford invariants of ade coxeter elements. *Advances in Applied Clifford Algebras*, 34(3):20, 2024.
- [30] David Ruhe, Johannes Brandstetter, and Patrick Forré. Clifford group equivariant neural networks. In *Thirty-seventh Conference on Neural Information Processing Systems*, 2023.
- [31] Johann Brehmer, Pim de Haan, Sönke Behrends, and Taco S Cohen. Geometric algebra transformer. In *Advances in Neural Information Processing Systems*, pages 35472–35496, 2023.
- [32] Zbigniew Oziewicz. The dirac operator as graph and the clifford hopf-gebra. *PITMAN RESEARCH NOTES IN MATHEMATICS SERIES*, pages 210–224, 1998.
- [33] William E Baylis. *Clifford (Geometric) Algebras: with applications to physics, mathematics, and engineering*. Springer Science & Business Media, 2012.
- [34] Leo Dorst, Daniel Fontijne, and Stephen Mann. Geometric algebra for computer science (revised edition). The Morgan Kaufmann Series in Computer Graphics. Morgan Kaufmann, 2009.
- [35] Pertti Lounesto. *Clifford Algebras and Spinors*. London Mathematical Society Lecture Note Series. Cambridge University Press, 2 edition, 2001.
- [36] Beata Casiday, Ivan Contreras, Thomas Meyer, Sabrina Mi, and Ethan Spingarn. Laplace and dirac operators on graphs. *Linear and Multilinear Algebra*, pages 325–365, 2024.
- [37] Mohammad Mahmudul Alam, Edward Raff, Stella Biderman, Tim Oates, and James Holt. Recasting self-attention with holographic reduced representations. In Andreas Krause, Emma Brunskill, Kyunghyun Cho, Barbara Engelhardt, Sivan Sabato, and Jonathan Scarlett, editors, *Proceedings of the 40th International Conference on Machine Learning*, volume 202 of *Proceedings of Machine Learning Research*, pages 490–507. PMLR, 23–29 Jul 2023. URL <https://proceedings.mlr.press/v202/alam23a.html>.
- [38] Ashwinkumar Ganesan, Hang Gao, Sunil Gandhi, Edward Raff, Tim Oates, James Holt, and Mark McLean. Learning with holographic reduced representations. In M. Ranzato, A. Beygelzimer, Y. Dauphin, P.S. Liang, and J. Wortman Vaughan, editors, *Advances in Neural Information Processing Systems*, volume 34, pages 25606–25620. Curran Associates, Inc., 2021. URL https://proceedings.neurips.cc/paper_files/paper/2021/file/d71dd235287466052f1630f31bde7932-Paper.pdf.
- [39] Matthias Wolff, Günther Wirsching, Markus Huber, Peter beim Graben, Ronald Römer, and Ingo Schmitt. A fock space toolbox and some applications in computational cognition. In Alexey Karpov, Oliver Jokisch, and Rodmonga Potapova, editors, *Speech and Computer*, pages 757–767, Cham, 2018. Springer International Publishing. ISBN 978-3-319-99579-3.
- [40] Avrim Blum, John Hopcroft, and Ravindran Kannan. *Foundations of Data Science*. Cambridge University Press, 2020.
- [41] Jacob Devlin, Ming-Wei Chang, Kenton Lee, and Kristina Toutanova. BERT: Pre-training of deep bidirectional transformers for language understanding. In Jill Burstein, Christy Doran, and Tamar Solorio, editors, *Proceedings of the 2019 Conference of the North American Chapter of the Association for Computational Linguistics: Human Language Technologies, Volume 1 (Long and Short Papers)*, pages 4171–4186, Minneapolis, Minnesota, June 2019. Association for Computational Linguistics. doi: 10.18653/v1/N19-1423. URL <https://aclanthology.org/N19-1423>.

- [42] Yinhan Liu, Myle Ott, Naman Goyal, Jingfei Du, Mandar Joshi, Danqi Chen, Omer Levy, Mike Lewis, Luke Zettlemoyer, and Veselin Stoyanov. Roberta: A robustly optimized bert pretraining approach. *arXiv preprint arXiv:1907.11692*, 2019.
- [43] Kenny Schlegel, Peer Neubert, and Peter Protzel. A comparison of vector symbolic architectures. *Artificial Intelligence Review*, 55, 08 2022. doi: 10.1007/s10462-021-10110-3.
- [44] T.A. Plate. Holographic reduced representations. *IEEE Transactions on Neural Networks*, 6(3): 623–641, 1995. doi: 10.1109/72.377968.
- [45] Yanli Zhao, Andrew Gu, Rohan Varma, Liang Luo, Chien-Chin Huang, Min Xu, Less Wright, Hamid Shojanazeri, Myle Ott, Sam Shleifer, Alban Desmaison, Can Balioglu, Pritam Damania, Bernard Nguyen, Geeta Chauhan, Yuchen Hao, Ajit Mathews, and Shen Li. Pytorch fsdp: Experiences on scaling fully sharded data parallel. *Proc. VLDB Endow.*, 16(12):3848–3860, aug 2023. ISSN 2150-8097. doi: 10.14778/3611540.3611569. URL <https://doi.org/10.14778/3611540.3611569>.
- [46] William L. Hamilton, Rex Ying, and Jure Leskovec. Inductive representation learning on large graphs. In *Proceedings of the 31st International Conference on Neural Information Processing Systems, NIPS’17*, page 1025–1035, Red Hook, NY, USA, 2017. Curran Associates Inc. ISBN 9781510860964.
- [47] Renming Liu and Arjun Krishnan. Open biomedical network benchmark: A python toolkit for benchmarking datasets with biomedical networks. In David A. Knowles and Sara Mostafavi, editors, *Proceedings of the 18th Machine Learning in Computational Biology meeting*, volume 240 of *Proceedings of Machine Learning Research*, pages 23–59. PMLR, 30 Nov–01 Dec 2024. URL <https://proceedings.mlr.press/v240/liu24a.html>.
- [48] James Dunbar, Konrad Krawczyk, Jinwoo Leem, Terry Baker, Angelika Fuchs, Guy Georges, Jiye Shi, and Charlotte M. Deane. SAbDab: the structural antibody database. *Nucleic Acids Research*, 42, 2013. ISSN 0305-1048. doi: 10.1093/nar/gkt1043. URL <https://doi.org/10.1093/nar/gkt1043>.
- [49] Hugo Touvron, Louis Martin, Kevin Stone, Peter Albert, Amjad Almahairi, Yasmine Babaei, Nikolay Bashlykov, Soumya Batra, Prajjwal Bhargava, Shruti Bhosale, et al. Llama 2: Open foundation and fine-tuned chat models. *arXiv preprint arXiv:2307.09288*, 2023.
- [50] Joan Bruna, Wojciech Zaremba, Arthur Szlam, and Yann Lecun. Spectral networks and locally connected networks on graphs. In *International Conference on Learning Representations (ICLR2014), CBLIS, April 2014*, 2014.
- [51] Zhiyuan Liu and Jie Zhou. *Graph Attention Networks*, pages 39–41. Springer International Publishing, Cham, 2020. ISBN 978-3-031-01587-8. doi: 10.1007/978-3-031-01587-8_7. URL https://doi.org/10.1007/978-3-031-01587-8_7.
- [52] Weihua Hu, Matthias Fey, Marinka Zitnik, Yuxiao Dong, Hongyu Ren, Bowen Liu, Michele Catasta, and Jure Leskovec. Open graph benchmark: datasets for machine learning on graphs. In *Proceedings of the 34th International Conference on Neural Information Processing Systems, NIPS ’20*, Red Hook, NY, USA, 2020. Curran Associates Inc. ISBN 9781713829546.
- [53] Seongjun Yun, Minbyul Jeong, Sungdong Yoo, Seunghun Lee, Sean S. Yi, Raehyun Kim, Jaewoo Kang, and Hyunwoo J. Kim. Graph transformer networks: Learning meta-path graphs to improve gnns. *Neural Networks*, 153:104–119, 2022. ISSN 0893-6080. doi: <https://doi.org/10.1016/j.neunet.2022.05.026>. URL <https://www.sciencedirect.com/science/article/pii/S0893608022002003>.
- [54] Petar Veličković, William Fedus, William L. Hamilton, Pietro Liò, Yoshua Bengio, and Devon Hjelm. Deep graph infomax. In *ICLR 2019*, May 2019. URL <https://www.microsoft.com/en-us/research/publication/deep-graph-infomax/>.
- [55] Yanqiao Zhu, Yichen Xu, Feng Yu, Qiang Liu, Shu Wu, and Liang Wang. Deep graph contrastive representation learning. *arXiv preprint arXiv:2006.04131*, 2020.

- [56] Hongyang Gao, Zhengyang Wang, and Shuiwang Ji. Large-scale learnable graph convolutional networks. In *Proceedings of the 24th ACM SIGKDD International Conference on Knowledge Discovery & Data Mining*, KDD '18, page 1416–1424, New York, NY, USA, 2018. Association for Computing Machinery. ISBN 9781450355520. doi: 10.1145/3219819.3219947. URL <https://doi.org/10.1145/3219819.3219947>.
- [57] Ming Chen, Zhewei Wei, Zengfeng Huang, Bolin Ding, and Yaliang Li. Simple and deep graph convolutional networks. In Hal Daumé III and Aarti Singh, editors, *Proceedings of the 37th International Conference on Machine Learning*, volume 119 of *Proceedings of Machine Learning Research*, pages 1725–1735. PMLR, 13–18 Jul 2020. URL <https://proceedings.mlr.press/v119/chen20v.html>.
- [58] Franco Scarselli, Marco Gori, Ah Chung Tsoi, Markus Hagenbuchner, and Gabriele Monfardini. The graph neural network model. *IEEE Transactions on Neural Networks*, 20(1):61–80, 2009. doi: 10.1109/TNN.2008.2005605.
- [59] Lingfei Wu, Peng Cui, Jian Pei, Liang Zhao, and Xiaojie Guo. Graph neural networks: Foundation, frontiers and applications. In *Proceedings of the 28th ACM SIGKDD Conference on Knowledge Discovery and Data Mining*, KDD '22, page 4840–4841, New York, NY, USA, 2022. Association for Computing Machinery. ISBN 9781450393850. doi: 10.1145/3534678.3542609. URL <https://doi.org/10.1145/3534678.3542609>.
- [60] Vijay Prakash Dwivedi and Xavier Bresson. A generalization of transformer networks to graphs. *arXiv preprint arXiv:2012.09699*, 2020.
- [61] Taco Cohen, Maurice Weiler, Berkay Kicanaoglu, and Max Welling. Gauge equivariant convolutional networks and the icosahedral CNN. In Kamalika Chaudhuri and Ruslan Salakhutdinov, editors, *Proceedings of the 36th International Conference on Machine Learning*, volume 97 of *Proceedings of Machine Learning Research*, pages 1321–1330. PMLR, 09–15 Jun 2019. URL <https://proceedings.mlr.press/v97/cohen19d.html>.
- [62] Michael M Bronstein, Joan Bruna, Taco Cohen, and Petar Veličković. Geometric deep learning: Grids, groups, graphs, geodesics, and gauges. *arXiv preprint arXiv:2104.13478*, 2021.
- [63] Monami Banerjee, Rudrasis Chakraborty, Jose Bouza, and Baba C. Vemuri. Volterraret: A higher order convolutional network with group equivariance for homogeneous manifolds. *IEEE Trans. Pattern Anal. Mach. Intell.*, 44(2):823–833, feb 2022. ISSN 0162-8828. doi: 10.1109/TPAMI.2020.3035130. URL <https://doi.org/10.1109/TPAMI.2020.3035130>.
- [64] Xuanyu Zhu, Yi Xu, Hongteng Xu, and Changjian Chen. Quaternion convolutional neural networks. In Vittorio Ferrari, Martial Hebert, Cristian Sminchisescu, and Yair Weiss, editors, *Computer Vision – ECCV 2018*, pages 645–661, Cham, 2018. Springer International Publishing. ISBN 978-3-030-01237-3.
- [65] Marc Finzi, Samuel Stanton, Pavel Izmailov, and Andrew Gordon Wilson. Generalizing convolutional neural networks for equivariance to lie groups on arbitrary continuous data. In Hal Daumé III and Aarti Singh, editors, *Proceedings of the 37th International Conference on Machine Learning*, volume 119 of *Proceedings of Machine Learning Research*, pages 3165–3176. PMLR, 13–18 Jul 2020. URL <https://proceedings.mlr.press/v119/finzi20a.html>.
- [66] Maksim Zhdanov, David Ruhe, Maurice Weiler, Ana Lucic, Johannes Brandstetter, and Patrick Forré. Clifford-steerable convolutional neural networks. *arXiv preprint arXiv:2402.14730*, 2024.
- [67] Marco A. S. Trindade, Vinícius N. A. Lula-Rocha, and S. Floquet. Clifford Algebras, Quantum Neural Networks and Generalized Quantum Fourier Transform. *Adv. Appl. Clifford Algebras*, 33(3):38, 2023. doi: 10.1007/s00006-023-01279-7.
- [68] P Erdős and A Rényi. On random graphs i. *Publicationes Mathematicae Debrecen*, pages 290–297, 1959.

- [69] Réka Albert and Albert-László Barabási. Statistical mechanics of complex networks. *Rev. Mod. Phys.*, 74:47–97, Jan 2002. doi: 10.1103/RevModPhys.74.47.
- [70] Fan Chung and Linyuan Lu. The average distances in random graphs with given expected degrees. *Proceedings of the National Academy of Sciences*, 99(25):15879–15882, 2002. doi: 10.1073/pnas.252631999. URL <https://www.pnas.org/doi/abs/10.1073/pnas.252631999>.
- [71] David B. Jaffe, Payam Shahi, Bruce A. Adams, Ashley M. Chrisman, Peter M. Finnegan, Nandhini Raman, Ariel E. Royall, Funien Tsai, Thomas Vollbrecht, Daniel S. Reyes, and Wyatt J. McDonnell. Functional antibodies exhibit light chain coherence. *Nature*, 611:352 – 357, 2022. URL <https://api.semanticscholar.org/CorpusID:248421668>.
- [72] Chris Stark, Bobby-Joe Breitkreutz, Teresa Reguly, Lorrie Boucher, Ashton Breitkreutz, and Mike Tyers. Biogrid: a general repository for interaction datasets. *Nucleic acids research*, 34 (Database issue):D535–9, January 2006. ISSN 0305-1048. doi: 10.1093/nar/gkj109. URL <https://europepmc.org/articles/PMC1347471>.
- [73] Sohyun Hwang, Chan Yeong Kim, Sunmo Yang, Eiru Kim, Traver Hart, Edward M. Marcotte, and Insuk Lee. Humannet v2: Human gene networks for disease research. *Nucleic acids research*, 47(D1):D573–D580, January 2019. ISSN 0305-1048. doi: 10.1093/nar/gky1126. Publisher Copyright: © 2018 The Author(s).
- [74] William Falcon and The PyTorch Lightning team. PyTorch Lightning, March 2019. URL <https://github.com/Lightning-AI/lightning>.
- [75] Zhenqin Wu, Bharath Ramsundar, Evan N Feinberg, Joseph Gomes, Caleb Geniesse, Aneesh S Pappu, Karl Leswing, and Vijay Pande. Moleculenet: a benchmark for molecular machine learning. *Chemical science*, 9(2):513–530, 2018.
- [76] Nick Erickson, Jonas Mueller, Alexander Shirkov, Hang Zhang, Pedro Larroy, Mu Li, and Alexander Smola. Autogluon-tabular: Robust and accurate automl for structured data. *arXiv preprint arXiv:2003.06505*, 2020.
- [77] David Rogers and Mathew Hahn. Extended-connectivity fingerprints. *Journal of Chemical Information and Modeling*, 50(5):742–754, 2010. doi: 10.1021/ci100050t. URL <https://doi.org/10.1021/ci100050t>. PMID: 20426451.
- [78] Jung-Hoon Han, Sarah Batey, Adrian A Nickson, Sarah A Teichmann, and Jane Clarke. The folding and evolution of multidomain proteins. *Nature reviews. Molecular cell biology*, page 319–330, 2007. ISSN 1471-0072. doi: 10.1038/nrm2144. URL <https://doi.org/10.1038/nrm2144>.

The code can be found in <https://anonymous.4open.science/r/FoGE>

A Dataset details

In our experiments, we used the following datasets:

1. **GraphQA** [15]: It includes 6 different graph-understanding tasks (*number of nodes, number of edges, cycle existence, number of triangles, node degree, and edge existence*) on 7 different graph structures (Erdos-Renyi [68], Scale-Free, Barabasi-Albert [69], Stochastic Block Model, Star, Path and Complete).
2. **GraphReasoning** [17]: Recently introduced in [17] to better assess the model’s graph understanding ability, it consists of 4 more advanced graph-understanding tasks (*substructure count, maximum triplet sum, shortest path, and bipartite graph matching*). Each graph node is accompanied by extra information in the form of a text description, making this dataset a suitable testbed for our RoBERTa-based vector encoding.
3. **HyperGraphQA**: We extend GraphQA to Hypergraphs. Specifically, we consider 4 different graph-understanding tasks (*number of nodes, number of edges, node degree, and edge existence*) on 2 different hypergraph structures (Erdos-Renyi [68], and Chung-Lu [70]). The training dataset consists of only 2000 instances, making it hard for large models to avoid overfitting.
4. **Jaffe** [71]: Jaffe is a recent dataset consisting of approximately 1.6 million natively paired human antibody sequences from healthy donors. To our knowledge, this represents by far the largest publicly available dataset of its kind.
5. **PPI** [46]: PPI consists of 24 proteins collected from human tissue, with each node associated with 121 binary labels. Compiled from experimental techniques like yeast two-hybrid screening and mass spectrometry, as well as computational predictions, such a dataset provides critical insights into the functional organization of the proteome. By understanding how proteins interact, scientists can uncover the molecular underpinnings of cellular processes and develop targeted therapeutic strategies.
6. **OBNB** [47]: OBNB (Open Biomedical Network Benchmark) is a collection of 15 datasets (including well-known datasets such as BioGRID [72] and HumanNet [73]). Each dataset’s sample consists of a gene accompanied by 3 vectors (named *DISEASES*, *DisGeNET*, *GOBP*) of node-level binary labels.
7. **SabDab** [48]: SabDab (Structural Antibody Database) is a collection of 919 publicly available, annotated antibody structures (proteins). Each structure is accompanied by multiple annotations, such as the heavy and light chain pairing.

B FoGE-LLM

B.1 Training details

We train the LLM-based construction with a batch size of 16 and a learning rate of $1e-3$. The model required less than 10 epochs to convergence, in contrast to other works that require more training time due to the elaborate graph encoders (e.g., [17]). Our implementation is based on Pytorch Lightning [74], which allows us to split and train the model on multiple GPUs using FSDP. This implementation allows the user to train this, or any similar, model to conventional GPUs with less memory while, at the same time, speed up the process by preloading all the obtained lightweight graph embeddings to the GPUs. The *merging* of the graph embedding with the LLM is based on the idea of prefix tuning [18], i.e., pre-append the embedding to the input text embeddings and, in our case, this is happening with the use of a linear adapter. We experimented both with a single linear adapter on the input layer, as well as a linear adapter per layer and the difference was only marginal in the final results.

B.2 Inference details

Besides the low training time, FoGE-LLM enjoys an extremely low inference time, due to two reasons. First, we always “reserve” only a single token for the provided graph. In contrast, zero/few-shot

approaches that textualize the graph require a large number of tokens, prohibitively large as the graph grows. This leads to an explosion of the inference time, due to the transformer’s quadratic dependency on the number of input tokens. Second, FoGE-LLM employs one or more linear adapters and does not require any specialized architectures, like existing solutions [17, 16]. This, as we observed in our experiments, impacts the inference time, casting FoGE-LLM one of the fastest graph-augmented Language Models. In Table 6 we present the average inference time required for each approach.

Table 6: Average inference time for each approach on Llama-7B. FoGE-LLM is significantly lower than zero/few shot approaches since the number of input tokens does not grow with the graph size, while it enjoys a 40% improvement over GraphLLM dues to its simpler encoder/adapter.

Model	Inference time (s) ↓
zero-shot	0.175 (± 0.05)
few-shot	0.541 (± 0.10)
GraphLLM [17]	0.052 (± 0.01)
FoGE-LLM	0.031 (± 0.01)

C ICL prompting for hypergraphs

In Table 5 we demonstrate FoGE’s superiority over In-Context Learning approaches, like zero-shot and few-shot prompting. Here we explain how we created the textual descriptions of the hypergraphs, that were used in both zero- and few-shot prompting. Following similar works for graph textualization [16, 15], we first assign a number to each node and then, in a new line, we explain which nodes are part of each hyperedge. An example can be seen below.

G describes a hypergraph among 0, 1, 2, 3, 4, 5, 6, 7, and 8.
 In this hypergraph:
 Hyperedge 1 connects nodes 2, 3, 6.
 Hyperedge 2 connects nodes 1, 4, 5, 7.
 Hyperedge 3 connects nodes 1, 2.
 Hyperedge 4 connects nodes 3, 5, 7, 8.

After the hypergraph textualization, the question follows in the case of zero-shot, while both the question and the answer follow in the case of few-shot.

D Lossless representations

One advantage of the obtained embeddings is that fact that the underlying structures are recoverable. This allows us to obtain unbiased vector estimates of complicated structures, such as graphs with multiple edge and node attributes. Here, we show how this property manifests in our specific formulation as well as more generally for pairs of key-item.

D.1 Capacity

One of the typical ways to examine the performance of such a construction is by assuming a vector \mathbf{u} as being the bundling of multiple binded pairs, as in the following equation

$$\mathbf{u} = \bigoplus_{i=1}^n \mathbf{k}_i \otimes \mathbf{v}_i \quad (5)$$

and then examine how accurately we can recover each vector \mathbf{v}_i , given the corresponding \mathbf{k}_i . In theory, the vector \mathbf{v}_i can be easily recovered using the operation:

$$\hat{\mathbf{v}}_i = \mathbf{k}_i^{-1} \otimes \mathbf{u} \quad (6)$$

In Fig. 6 we examine the cosine similarity of the obtain vector $\hat{\mathbf{v}}_i$ with the correct one (\mathbf{v}_i) as well as with all the rest ($\{\mathbf{v}_j\}_{j \neq i}$). We observe that the results follow closely the theoretical results above, with a perfect separation of up to 100 pairs, and a small overlap for 200 – 300 pairs of vectors.

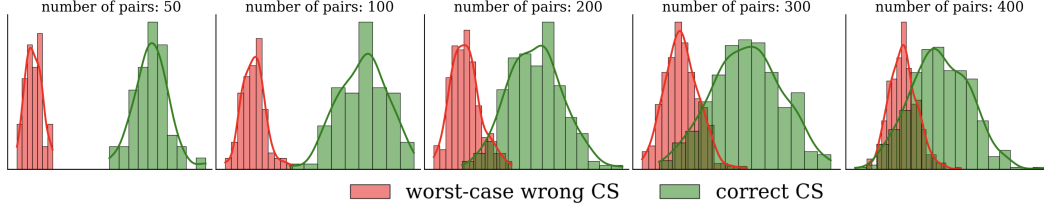


Figure 6: Given a vector $\mathbb{R}^{4096} \ni \mathbf{u} = \bigoplus_{i=1}^n \mathbf{k}_i \otimes \mathbf{v}_i$, how correctly we can recover all pairs of keys-values back, as the number of pairs (n) grows. *Worst-case wrong CS* corresponds to the maximum cosine similarity of the recovered value vector with all value vectors but the correct one, and *correct CS* corresponds to the cosine similarity with the correct value vector.

D.2 Graph reconstruction

In our specific application, we deal with graphs and, as we analyzed, the graph representations we obtain are, in theory, lossless, i.e., we can recover back the original graph from the vector representation using the inverse vectors. Here, we examine whether this claim holds in practice too. In Fig. 7 you can observe the strength of each edge after reconstruction, for 3 different vector dimensionalities. We can observe that, even for a moderately large dimension, there is a clear separation between the true edge set and the rest of the edges.

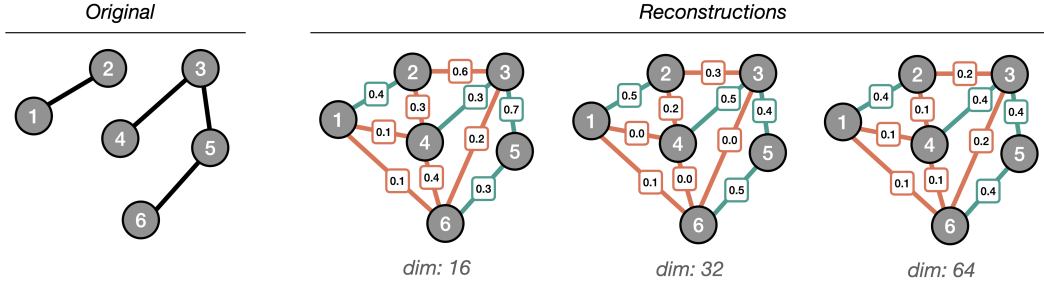


Figure 7: Lossless representations: even for small vector dimension, we can obtain back the true edge set. The numbers show the cosine similarity of the obtained vector with the true edge vector, and it can be used to estimate the true edge set.

E Graph understanding tasks

E.1 Basic graph understanding

Given the theoretical guarantees of the encoding procedure, initially we assess its practical strengths by first encoding graphical structures from 3 different classes of graphs (graphs, hypergraphs, and proteins) and then training small neural networks (one hidden layer) to predict graph attributes like *number of nodes* and *edges*. In Table 7 we show the performance. The results indicate that our representations are rich and informative and only few parameters suffice to achieve almost-perfect performance on such tasks.

Table 7: Using a small neural network with a single layer on the obtained graph representations allows us to perform almost perfectly in tasks such as *number of nodes* and *number of edges* in a graph, for both synthetic and real data.

	GraphQA			HyperGraphQA		Jaffe	
	num nodes	num edges	has cycle	num nodes	num edges	num acids	num links
MSE/Acc	0.67	0.03	98.7%	1.12	0.63	2.95	11.9
Model size	32K	8K	16K	32K	4K	32K	16K

E.2 Advanced graph understanding

After having demonstrated that relatively simple questions about graphs, such as the number of nodes and cycle existence, can be answered with almost perfect accuracy, we examine whether we can use the same encoding for more convoluted, real-life graphs. Specifically, we consider the mol-HIV dataset [75] from OGB [52] and, in Table 8, we demonstrate that our encoding can lead to results better than multiple, trainable methods. To obtain the final results we used AutoGluon [76] on our unsupervised embeddings, with a time limit of 10 minutes. Additionally, the addition of molecular fingerprints, as obtained by [77], can further strengthen the results and place us in the top-5 of all-time submissions.

Table 8: Results on mol-HIV [75, 52]. The full details of each model and the leaderboard can be found on https://ogb.stanford.edu/docs/leader_graphprop

	ROC-AUC
HyperFusion	0.8475 ± 0.0003
PAS + Fingerprint	0.8420 ± 0.0015
HIG	0.8403 ± 0.0021
DeepAUC	0.8352 ± 0.0054
FoGE + Fingerprint	0.8305 ± 0.0068
GMAN + Fingerprint	0.8244 ± 0.0033
RF + Fingerprint	0.8208 ± 0.0037
FoGE	0.7614 ± 0.0051
GCN	0.7606 ± 0.0097
GIN	0.7558 ± 0.0140

F Preservation of Clade information on SabDab

Given that the SabDab proteins [48] are annotated with the heavy/light chain pairing, we can extract the clades and visualize their embeddings with respect to that information. As a brief reminder, the clades correspond to superfamilies of proteins that share a common ancestor [78]. To extract the clades we used the V gene heavy chain and chose seven families. It is well known from biology that antibodies that belong to the same clade are *more similar* than antibodies across different clades, so, here, we examine if this real-world, biological property is reflected on our embeddings. Specifically, after obtaining each protein’s embedding using FoGE (in an unsupervised fashion without using the clade annotations), we apply a T-SNE transformation on the high-dimensional vectors so that we are able to plot them, with a significant amount of noise, in just two dimensions. Although we reduce the dimensionality significantly, and, even worse, we deal with a extremely small dataset of just 919 proteins (Table 9), in Fig. 8 we can observe that the proteins of each clade cluster together. This is a different, qualitative indicator, which shows that FoGE is able to preserve all the information that is encapsulated in the inputted structures.

Table 9: Distribution of samples across the different clades. In total there are 919 samples, with clades 1, 3, 4 being the most frequent.

Clade	1	2	3	4	5	6	7	Total
Count	325	28	414	101	25	3	23	919

G Additional results on OBNB

OBNB (which stands for Open Biomedical Network Benchmark) is a collection of multiple, real-world protein datasets, where each node (or amino-acid) of each protein is accompanied by multiple binary labels. A detailed analysis of the datasets and their labels can be found in [47] and the corresponding repository. In Table 10 we present the results on all 18 reported datasets of OBNB. FoGE is one of the best-performing methods across all benchmarks, showcasing once more the capabilities of our obtained embeddings.

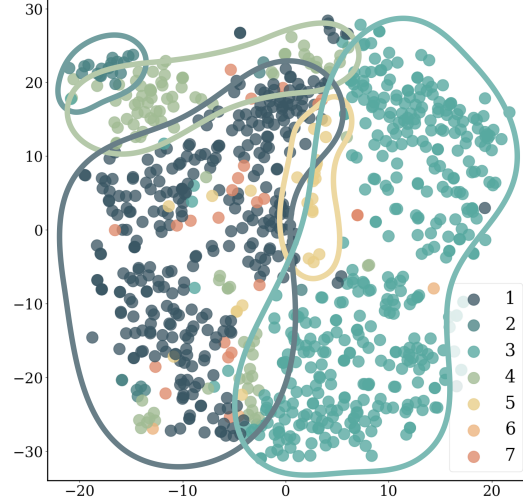


Figure 8: T-SNE plot of the SabDab embeddings. Although the dataset is very small, each one of the populated clades occupies a different region and, interestingly, clades 1 and 7 are very similar, just like in real life. The T-SNE plot was robust to different choices of hyperparameters, with no significant differences beyond simple translations of the space.

H Impact of vector dimension

One of few the hyperparameters of FoGE is the dimensionality of the vectors (i.e. graph embeddings). Using GraphQA, we perform an ablation study on the impact of the dimension on the final accuracy of the model (Fig. 9). Relative accuracy is calculated as the actual accuracy for each dimensionality, divided by the best one, for each task respectively, and it allows us to compare different tasks with completely different best performances (Table Table 3).

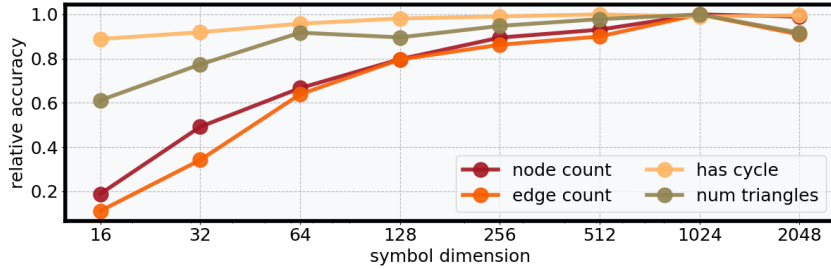


Figure 9: Accuracy versus vectors dimensionality. Although there is a positive trend between the two quantities, the dependency on the dimension is not equally strong or always positive in all tasks.

From this study, a few important remarks surface that we observe to hold true for the other datasets too. First of all, a larger dimensionality does not always “translate” to better results. We observe that for some tasks (*cycle existence*), we achieve the optimal performance with a dimension significantly lower than the maximum we consider (2048), matching essentially GraphToken’s performance with less than 20K trainable parameters, while in some cases there is a small drop as we go from 1024 to 2048. Finally, as with most of the tunable hyperparameters in machine learning models, there is no predetermined best strategy for choosing the dimensionality. For instance, when we consider *cycle existence* or *the number of triangles* we can have a highly performing model with a dimensionality of less than 128, while for tasks such as *edge* and *node count* the performance drops significantly as we reduce the dimensionality.

Table 10: FoGE vs multiple unsupervised and supervised methods. After obtaining our embeddings, we use a Random Forest to predict the corresponding node’s label. The evaluation is based on the APOP metric [47] and we can observe that FoGE is always comparable to the best methods, while in almost half of the cases it is the best one.

Network	Model	DISEASES	DisGeNET	GOBP
BioGRID	LabelProp	1.210	0.931	1.858
	LogReg	1.556	1.026	2.571
	GCN+BoT	1.511	1.014	2.442
	SAGE+BoT	1.486	1.031	2.402
	GIN+BoT	1.410	1.007	2.386
	GAT+BoT	1.609	1.037	2.624
	GatedGCN+BoT	1.547	1.038	2.517
	FoGE	1.599	1.062	2.433
HumanNet	LabelProp	3.728	3.098	3.806
	LogReg	3.812	3.158	4.053
	GCN+BoT	3.552	3.053	3.921
	SAGE+BoT	3.401	3.052	3.816
	GIN+BoT	3.513	3.054	3.861
	GAT+BoT	3.761	3.100	3.809
	GatedGCN+BoT	3.677	3.086	3.889
	FoGE	3.853	3.254	3.916
COMPPIHumanInt	LabelProp	1.352	1.106	2.076
	LogReg	1.644	1.240	2.806
	GCN+BoT	1.648	1.211	2.685
	SAGE+BoT	1.694	1.210	2.629
	GIN+BoT	1.608	1.219	2.611
	GAT+BoT	1.665	1.230	2.755
	GatedGCN+BoT	1.672	1.218	2.735
	FoGE	1.660	1.241	2.586
BioPlex	LabelProp	0.964	0.939	1.714
	LogReg	1.358	0.939	2.587
	GCN+BoT	1.324	0.911	2.553
	SAGE+BoT	1.246	0.865	2.513
	GIN+BoT	1.349	0.868	2.504
	GAT+BoT	1.355	0.873	2.548
	GatedGCN+BoT	1.301	0.859	2.590
	FoGE	1.273	0.879	2.599
HuRI	LabelProp	0.545	0.598	1.086
	LogReg	0.650	0.656	1.084
	GCN+BoT	0.634	0.693	1.129
	SAGE+BoT	0.593	0.679	1.190
	GIN+BoT	0.583	0.702	1.143
	GAT+BoT	0.667	0.687	1.174
	GatedGCN+BoT	0.596	0.695	1.195
	FoGE	0.684	0.729	1.070
OmniPath	LabelProp	1.358	0.897	1.593
	LogReg	1.542	1.093	2.125
	GCN+BoT	1.577	1.068	2.071
	SAGE+BoT	1.478	1.062	1.986
	GIN+BoT	1.452	1.073	1.993
	GAT+BoT	1.552	1.048	2.068
	GatedGCN+BoT	1.516	1.049	2.071
	FoGE	1.511	1.085	2.102